Biogeosciences Discuss., https://doi.org/10.5194/bg-2019-11
Manuscript under review for journal Biogeosciences
Discussion started: 22 January 2019

Rhizosphere to the atmosphere: contrasting methane pathways, fluxes and geochemical drivers across the terrestrial-aquatic wetland boundary

Luke C. Jeffrey[1,2], Damien T. Maher[1,2,3], Scott Johnston[1], Kylie Maguire[1], Andrew D.L. Steven[4] and Douglas R. Tait[1,2].

[1]SCU Geoscience, Southern Cross University, PO Box 157, Lismore, NSW 2480, Australia.

[2]National Marine Science Centre, Southern Cross University, PO Box 4321, Coffs Harbour, NSW 2450, Australia.

[3]School of Environment, Science and Engineering, Southern Cross University, Lismore, NSW 2480, Australia

[4]CSIRO Oceans and Atmosphere, Queensland Biosciences Precinct, University of Queensland, 306 Carmody Rd, St Lucia, Brisbane 4067, Australia

Corresponding author: luke.jeffrey@scu.edu.au

Key Words:

Diffusion

Ebullition

Sediment redox

Coastal acid sulphate soils

Sulphate reduction

Iron reduction

Carbon cycle

Biogeosciences Discuss., https://doi.org/10.5194/bg-2019-11
Manuscript under review for journal Biogeosciences
Discussion started: 22 January 2019

Abstract

Although wetlands represent the largest natural source of atmospheric CH_4, large uncertainties remain regarding the global CH_4 flux. Wetland hydrological oscillations contribute to this uncertainty, dramatically altering wetland area, water table height, soil redox potentials and CH_4 emissions. This study compares both terrestrial and aquatic CH_4 fluxes over two distinct seasons in both permanent and seasonal remediated freshwater wetlands in subtropical Australia. We account for aquatic CH_4 diffusion and ebullition rates, and plant-mediated CH_4 fluxes from three distinct vegetation communities, thereby examining seasonal, diurnal and intra-habitat variability. CH_4 emission rates were related to underlying sediment geochemistry. For example, distinct negative relationships between Fe(III) and SO_4^{2-} and CH_4 fluxes were observed, whereas distinct positive trends occurred between CH_4 emissions and Fe(II) / AVS, where sediment Fe(III) and SO_4^{2-} were depleted. The highest CH_4 emissions of the seasonal wetland were measured during flooded conditions and always during daylight hours, which is consistent with soil redox potential and temperature being important co-drivers of CH_4 flux. The highest CH_4 fluxes were consistently emitted from the permanent wetland (1.5 to 10.5 mmol m^{-2} d^{-1}), followed by the Phragmites australis community within the seasonal wetland (0.8 to 2.3 mmol m^{-2} d^{-1}), whilst the lowest CH_4 fluxes came from a region of forested Juncus sp. (-0.01 to 0.1 mmol m^{-2} d^{-1}) which also corresponded with the highest sedimentary Fe(III) and SO_4^{2-}. We suggest that wetland remediation strategies should consider geochemical profiles to help to mitigate excessive and unwanted methane emissions, especially during early system recovery periods.

Biogeosciences Discuss., https://doi.org/10.5194/bg-2019-11
Manuscript under review for journal Biogeosciences
Discussion started: 22 January 2019

1.0 Introduction

Wetlands are considered one of the most valuable ecosystems on Earth (Costanza et al., 2014). They are biodiversity hotspots that provide ecosystem services such as water filtration, sediment trapping, floodwater retention and carbon (C) storage (Bianchi, 2007). Wetlands account for ~5.5% of terrestrial surfaces (Melton et al., 2013) and have been estimated to store from ~4% (Bridgham et al., 2014) to ~30% (Mitsch et al., 2013) of Earth's estimated 2500 Pg soil C pool (Lal, 2008). Pristine wetlands have long been considered net C sinks due to their high rates of productivity and low rates of decomposition (Mitsch et al., 2013); however due to their waterlogged nature and anaerobic soils, wetlands are ideal environments for the production of methane (CH_4), a potent greenhouse gas. As such, wetlands are recognised as Earth's largest natural source of CH_4 to the atmosphere (185 ± 21 Tg C yr^{-1}) (Saunois et al., 2016).

Resolving the drivers, pathways and effects of seasonal weather oscillations on wetland CH_4 sink or source behaviours is important to enable more accurate climate model projections and to reduce uncertainties in the global wetland CH_4 budget (Kirschke et al., 2013; Saunois et al., 2016). Mitsch et al. (2013) estimated that the average ratio of freshwater wetland CO_2 sequestration to CH_4 emissions was 19.5:1. As CH_4 is 34 times more potent than carbon dioxide (CO_2) over a 100 year time scale (Stocker et al., 2013), this suggests that many freshwater wetlands may have a net positive radiative forcing effect on climate (Hernes et al., 2018). However, variability in geomorphology, wetland maturity, salinity and underlying geochemical composition all contribute to variable CH_4 dynamics (Bastviken et al., 2011; Poffenbarger et al., 2011; Whiting & Chanton, 2001). The lack of spatially-resolved wetland CH_4 emission data, as well as the limited number of studies constraining the multiple wetland CH_4 flux pathways (i.e. ebullition, diffusion and plant-mediated) coupled with ongoing anthropogenic conversion of wetland systems (Bartlett & Harriss, 1993; Neubauer & Megonigal, 2015; Saunois et al., 2016) further contribute to the uncertainties around CH_4 regional to global scale budgets.

Extensive clearing and drainage of many coastal wetlands has occurred over the previous two centuries in order to accomodate agriculture, aquaculture and urban development (Armentano & Menges, 1986; Villa & Bernal, 2018; White et al., 1997). Drained wetlands can lead to rapid soil organic matter oxidation, and transform systems to net CO_2 sources (Deverel et al., 2016; Pereyra & Mitsch, 2018). Drainage systems can also reduce wetland inundation

periods and alter sediment redox-dependant geochemistry and microbially-mediated reactions (Johnston et al., 2014), particularly those involving bioavailable iron (Fe(III)), sulphate (SO_4^{2-}) and nitrate (NO_3^-). Importantly, anaerobic carbon metabolism employing these terminal electron acceptors (Fe(III), SO_4^{2-}, NO_3^-) competes thermodynamically with methanogenic bacteria and archaea and thereby can inhibit CH_4 production (á Norði & Thamdrup, 2014; Burdige, 2012; Karimian et al., 2018; Lal, 2008). With increasing value now placed on the ecosystems services provided by wetlands, many degraded systems are now undergoing remediation and re-flooding (Johnston et al., 2014). However, the ecosystem benefits, such as enhanced biodiversity and water quality, may come at a price in the form of high initial CH_4 flux rates, and predicted net radiative forcing for several centuries post-remediation - thus posing a 'biogeochemical compromise' (Hemes et al., 2018; Lal, 2008).

Within Australia, it has been estimated that more than 50% of natural wetlands have been lost to land use change, drainage and degradation since European settlement (Finlayson & Rea, 1999; ANCA, 1995). This equates to an estimated ~1.2 Pg C emitted to the atmosphere through oxidation of soil organic carbon (Page & Dalal, 2011). Much of eastern Australia's freshwater coastal wetlands are underlain by Holocene derived sulphidic sediments (i.e pyrite – Fe_2S, known as coastal acid sulphate soils; CASS) formed during periods of higher sea levels (Walker, 1972; White et al., 1997). When CASS are drained, pyrite is oxidised, producing sulphuric acid (H_2SO_4). This results in highly acidic soils with pH levels as low as 3 (Johnston et al., 2014; Sammut et al., 1996). After rainfall events, groundwater transports H_2SO_4 from the CASS landscapes into nearby creeks and estuaries (Sammut et al., 1996). The low pH groundwater discharge also mobilises iron and aluminium, fuels aquatic deoxygenation, and can lead to large fish kills and degradation of infrastructure (Jeffrey et al., 2016; Johnston et al., 2003; White et al., 1997; Wong et al., 2010). Drained CASS wetlands typically contain abundant reactive Fe(III) and exhibit complex sulphur and Fe cycling (Boman et al., 2008; Burton et al., 2011; Burton et al., 2006). Wetland iron and sulfur cycling can profoundly influence CH_4 production and consumption via a series of complex redox reactions coupled with organic matter mineralisation (Holmkvist et al., 2011; Sivan et al., 2014). As such, terminal electron acceptor availability is critical when considering wetland remediation and the biogeochemical compromise paradigm.

Here we assess CH_4 emissions rates from a remediated freshwater CASS wetland in subtropical eastern Australia, and compare fluxes from the permanent wetland and the adjacent seasonal wetland ecotypes. We hypothesize that wetland CH_4 emissions will differ

Biogeosciences Discuss., https://doi.org/10.5194/bg-2019-11
Manuscript under review for journal Biogeosciences
Discussion started: 22 January 2019

significantly between the seasons and between the four wetland communities. We account for three atmospheric flux pathways for methane; ebullition, diffusion and plant-mediated fluxes, over diurnal cycles and within different seasons. CH_4 fluxes were also assessed in relation to the underlying soil properties, including sulphate, reactive iron III and iron II, acid volatile sulphur, chloride and organic carbon.

2.0 Methods

2.1 Study site

Cattai Wetland is located on the mid-coast of New South Wales, Australia. The reserve covers 500 hectares, featuring a shallow permanent wetland covering an area of approximately 16 hectares that is adjacent to a seasonal wetland and floodplain located to the south (Fig. 1). Both sites discharge into the nearby Coopernook Creek, a tributary of the larger Manning River estuary. The site was extensively cleared and low-lying areas drained during the early 1900's in order to aid agriculture and development in the region. As a result of this anthropogenic drainage, the oxidation of CASS produced sulphuric acid and episodic acidic discharge to adjacent creeks for many years (Tulau, 1999). To ameliorate acidic discharge, the natural hydrology of the site was restored in 2003 through the decommissioning of agricultural drains and removal of floodgates. Re-flooding of the CASS landscape has reduced the production of sulphuric acid, acid discharge and aluminium and iron mobilisation, hence improving the downstream water quality (GTCC, 2014).

The region receives a mean annual rainfall of 1180 mm with the majority falling during early autumn with an average maximal monthly rainfall in March (152 mm). The lowest rainfall generally occurs during the winter months with average minimal rainfall during September (60 mm). Average minimum and maximum summer temperatures range from 17.6 °C to 29 °C (January) and in winter range from 5.9 °C to 18.5 °C (July) (BOM, 2018). The dominant vegetation type within the permanent wetland is an introduced waterlily species (*Nymphaea capensis*), while the fringes of the wetland consist of wetland tree species; *Casuarina* sp. and *Melaleuca quinquenervia*. The seasonal wetland to the south is dominated by the sedge; *Juncus kraussii* (Veg A) and features scattered stands of *Phragmites australis* (Veg B) with areas of slightly higher elevation dominated by *Juncus kraussii* below *Casuarina sp.* (Veg C) (Fig. 1).

Biogeosciences Discuss., https://doi.org/10.5194/bg-2019-11
Manuscript under review for journal Biogeosciences
Discussion started: 22 January 2019

2.2 The aquatic CH_4 flux of the permanent wetland

To quantify CH_4 ebullition rates, up to 12 ebullition domes were deployed during two distinct seasons (detailed below) at ~20 m intervals along a longitudinal transect, from the edge of the permanent wetland towards the centre. Each dome was carefully suspended below the water level by flotation rings, ensuring minimal disturbance of sediment and the water column. Gas samples were extracted from the headspace of each dome using a 300 mL gas tight syringe at periods of ~48 h. The volume was recorded and each sample then diluted using ambient air (1:729 ratio) and analysed in situ using a using a manufacturer calibrated cavity ring-down spectrometer (Picarro G2201-*i*) to determine CH_4 concentrations (ppm). Diffusive CH_4 fluxes from the permanent wetland were measured using a floating chamber with a portable greenhouse gas analyser (UGGA, Los Gatos Research). To account for spatial and temporal variability, measurements were conducted during both day-time and night-time, and sampling within vegetated areas featuring lilies (*Nymphaea capensis*), forested areas (*Melaleuca* sp.) and in areas where no aquatic vegetation was present (i.e. open water). A total of 39 CH_4 floating chamber incubations averaging ~8 minutes in duration were recorded over the two campaigns. The average r^2 value of linear regressions of CH_4 concentrations versus time during chamber incubations was 0.97 ± 0.05. One chamber measurement was disregarded as an outlier (as it was more than three times the standard deviation of the mean) and any chambers capturing ebullition bubbles (determined by a nonlinear increase in concentration) were also disregarded. The seasonal ebullition and diffusive CH_4 flux methods and measurements from the permanent wetland have previously been reported elsewhere (Jeffrey et al. submitted).

2.3 Plant-mediated CH_4 fluxes

Simultaneous time series chamber experiments were conducted over ~24 hours to measure CH_4 fluxes during each season from the three different wetland vegetation ecotypes. These ecotypes were *Juncus kraussii* (Veg A), *Phragmites australis* (Veg B) and *Juncus kraussii* amongst *Casuarina sp.* forest (Veg C) (Fig. 1). In each ecotype, 65 x 65 x 30 cm acrylic bases were installed four months before the first time series experiment, to minimise disturbance to the sediment profile and vegetative rhizosphere. Vegetative flux chambers were constructed of an aluminium frame with clear Perspex walls and roof that matched the areal footprint of the pre-inserted acrylic bases. The chambers were 100 cm, 150 cm and 50 cm high for at Veg A, B and C respectively. The custom sizes were tailored for the different vegetation

Biogeosciences Discuss., https://doi.org/10.5194/bg-2019-11
Manuscript under review for journal Biogeosciences
Discussion started: 22 January 2019

heights, whilst minimising chamber volume as much as possible. Each chamber was leak-tested under laboratory conditions prior to fieldwork.

Before each field incubation, chambers were flushed with atmospheric air then carefully lowered over the vegetation and onto the acrylic base ensuring an air tight seal. A small fan circulated internal air within each chamber. Air within the chamber was pumped through a closed loop from the top of the chamber using gas tubing (Bevaline), passing through a drying agent (Drierite desiccant) and then analysed in situ using a calibrated cavity ring-down spectrometers (Picarro G2201-*i* or LosGatos), recording the flux rate of CH_4 (ppm/sec). The gas flow was returned near the base inside each vegetation chamber closing the loop. Vegetation incubation times ranged from 6 to 15 minutes depending on the flux rate and were taken from triplicate sites to account for heterogeneity within each ecotype. The daytime measurements (after sunrise) were measured at ~10 minute intervals whilst night time measurements (after sunset) were taken at ~4 hourly intervals. CH_4 fluxes from the adjacent exposed sediments or shallow overlying water at each site were also measured at ~4 hourly intervals to determine the influence and role of plant-mediated CH_4 fluxes compared to non-vegetated CH_4 fluxes. Light and temperature loggers (Onset Hobo) measured the changes in diurnal air temperature (°C) and photosynthetically active radiation (PAR) at each site.

2.4 Soil geochemistry and redox conditions

A water logger (Minidiver) was deployed in the permanent wetland before the first campaign to monitor changes in water depth (cm) and temperature (°C). Field pH (pH_F) and the redox potential (Eh_F; reported against standard hydrogen electrode) were determined in situ, by directly inserting the electrode into the soils (5 cm depth, 8 replicates) at each site. A composite sampling approach (3 cores) was used to collect sediment samples from each site, to determine organic C content, $Fe(III)_{HCl}$, $Fe(II)_{HCl}$, Cl, SO_4^{2-} and acid volatile sulphur (AVS). The cores were extracted in December 2016, by inserting a 4.0 cm diameter acrylic tube into the sediment to a depth of up to 50 cm. Cores were immediately sectioned into 2 cm increments to a depth of 20 cm, and 5 cm increments thereafter, ensuring higher vertical resolution in the organic rich near-surface sediments. Samples were immediately placed into air-tight bags, then frozen within 12 hr of collection at -16°C in a portable freezer and transferred to -80°C freezer in the laboratory. Frozen samples were thawed in an oxygen-free anaerobic chamber (1-5% H_2

in N_2), using an oxygen consuming palladium (Pd) catalyst. The defrosted samples were homogenised using a plastic spatula.

AVS content was determined by adding 1-2 g of wet sediment with 6 M HCl:1 M L-ascorbic acid. The liberated H_2S was captured in 5 ml of 3% Zn acetate in 2 M NaOH and then quantified using iodometric titration. The reactive Fe fractions were determined using a sequential extraction procedure optimised for acid sulphate soils based on Claff et al. (2010). Poorly crystalline solid-phase Fe (II) and Fe (III) were determined by extracting 2 g wet sub-samples with cold N_2-purged 1 M HCl for four hours. Aliquots of 0.45 µm-filtered extract were analysed for Fe (II) [$Fe(II)_{HCl}$] and total Fe [Fe_{HCl}] using the 1,10-phenanthroline method with the addition of hydroxylammonium chloride for total Fe (APHA, 2005). The Fe(III) [$Fe(III)_{HCl}$] was determined by the difference of [Fe_{HCl}] – [$Fe(II)_{HCl}$]. Total organic carbon (TOC) and total S (S_{Tot}) were determined via a LECO CNS-2000 carbon and sulfur analyser. Chloride and sulfate concentrations were measured using filtered (0.45 µm) aliquot from a 1:5 water extract of freshly defrosted wet soil, as per Rayment and Higginson (1992) via ion chromatography using a Metrosep A Supp4-250 column, an RP2 guard column and eluent containing 2 mM $NaHCO_3$, 2.4 mM Na_2CO_3 and 5% acetone, in conjunction with a Metrohm MSM module for background suppression.

2.5 Calculations

Both the air-water and vegetative CH_4 fluxes were calculated for the chamber deployments in the permanent wetland and seasonal wetland using the equation:

$$F = (s(V/RT_{air}A))t \quad (1)$$

where s is the regression slope for each chamber incubation deployments (ppm sec^{-1}), V is the chamber volume (m^3), R is the universal gas constant, T_{air} is the air temperature inside the chamber (K), A is the surface area of the chamber (m^2) and t is the conversion factor from seconds to day, and to mmol.

Ebullition rates (E_b) (mmol m^{-2} d^{-1}) were calculated using the equation:

$$E_b = ([CH_4].CH_{4Vol}.)/ A.V_m.Td \quad (2)$$

where [CH_4] is the CH_4 concentration in the collected gas (%), CH_{4Vol}. is the gas volume sampled (L), A is the funnel area (m^2), V_m is the molar volume of CH_4 at in situ temperature (L) and Td is deployment time (days).

3.0 Results

3.1 Hydrological Conditions

Prior to the first campaign in April 2017 (C1), an extreme hot/drying summer period occurred during early 2017 (Fig. 2). This resulted in an average wetland water column temperature of 23.3 ± 0.7 ºC and a water depth in the permanent wetland as low as ~7.3 cm, with exposed sediments along the wetland perimeter during the preceding month. Total rainfall for the two weeks prior to C1 was 342 mm, with an additional 35 mm of rain occurring during C1 fieldwork (Fig. 2) thus raising the water column depth in the permanent wetland to 77.2 cm in less than four weeks. This C1 deployment was therefore categorized as the 'post-dry/flooded' period, where air temperatures ranged from 13.3 to 22.8 ºC and the average water column temperature in the permanent wetland was 20.4 ± 0.5 ºC. The second fieldwork campaign was conducted in September 2017 (C2) under cool/drying conditions, where air temperatures ranged from as low as 3.4 ºC to 34.9 ºC (Fig. 2), with cooler average water temperatures 12.6 ± 0.4 ºC in the permanent wetland (Fig. 2). The depth of the permanent wetland at this time had dropped slightly to ~33 cm (Fig. 2).

3.2 Permanent and Seasonal Wetland CH_4 fluxes

The vegetation time series revealed diurnal variability of plant-mediated CH_4 emissions occurred at most ecotypes, with the highest CH_4 fluxes occurring during daytime around mid-day and the lowest CH_4 fluxes during the night time (Fig. 3, Table 1). The lowest CH_4 fluxes were found at Veg C with a net negative CH_4 flux observed during C2 time series. The CH_4 sediment fluxes measured amongst each vegetation time series were consistently much lower than the plant-mediated CH_4 fluxes indicating that the vegetation was indeed the main conduit for CH_4 to the atmosphere (Fig. 3, Table 1). The CH_4 fluxes were highly variable between the replicates at each site. Temperature and PAR followed similar diurnal trends to each other and had positive correlations to CH_4 emissions (Fig. 3).

Biogeosciences Discuss., https://doi.org/10.5194/bg-2019-11
Manuscript under review for journal Biogeosciences
Discussion started: 22 January 2019

263 CH_4 fluxes from the three vegetation types were higher in C1 than C2 (Fig. 4, Table 1).
264 The highest CH_4 fluxes in each of the vegetation types always occurred during the daytime
265 (Fig. 4, Table 1). *Phragmites sp.* (Veg B) consistently emitted the highest CH_4 fluxes (2.27 ±
266 1.42 mmol m^{-2} d^{-2} during C1 and 0.77 ± 0.46 mmol m^{-2} d^{-1} during C2). The Veg C ecotype
267 within the seasonal wetland consistently produced the lowest CH_4 fluxes of all sites, with a net
268 negative flux occurring during C2 (-0.01 ± 0.08 mmol m^{-2} d^{-1}).

269 The permanent wetland showed an inverse trend with seven-fold higher diffusive fluxes
270 during the cool/drying C2 (10.46 ± 15.81 mmol m^{-2} d^{-1}) compared to the post-dry/flooded C1
271 (1.49 ± 2.75 mmol m^{-2} d^{-1}), while the ebullition rates were similar during both seasons (Fig. 4,
272 Table 1). Overall, the plant mediated CH_4 fluxes from the three seasonal wetland vegetation
273 ecotypes (Veg A, B and C) were within the range of aquatic fluxes measured from the
274 permanent wetland for the post-dry/flooded C1 time series, but not for the cool/drying C2 time
275 series, when the permanent wetland CH_4 fluxes were much higher (Fig. 4).

276

277 **3.3 Sediment core profiles and soil redox potentials**

278 Average concentrations from soil cores (Table 1, Fig. 5) were based upon the top 20
279 cm of the profile, where the highest organic carbon concentrations were found. This upper
280 rhizosphere depth zone is assumed to be an active area of carbon metabolism and CH_4
281 production and consumption (Nedwell & Watson, 1995). The $Fe(III)_{HCl}$ concentrations were
282 greater than $Fe(II)_{HCl}$ at all three seasonal wetland sites, however the permanent wetland
283 showed an opposite trend with low concentrations of both Fe(III) (5.6 ± 10.7 mmol kg^{-1}) and
284 SO_4^{2-} (1.5 ± 1.0 mmol kg^{-1}) (Fig. 5, Table 1). The highest average concentrations of $Fe(III)_{HCl}$
285 were found at the Veg C site (204.0 mmol kg^{-1}) and highest and similar concentrations of SO_4^{2-}
286 were in Veg B and Veg C sediments (45.4 ± 41.0 mmol kg^{-1} and 43.3 ± 16.7 mmol kg^{-1}) (Fig.
287 5, Table 1). Net positive redox potential was found at all four sites during C1 (under post-dry/
288 flooded conditions) indicating a lag time between recent flooding and the onset of reducing
289 conditions. In contrast, a negative redox potential was found within the permanent wetland and
290 Veg B during C2, indicating reduced conditions under cool drying conditions (Table 1). The
291 TOC concentrations (%) were highest in the upper profiles and similar across all sites (Fig. 5,
292 Table 1) averaging 13.4 ± 7.6%.

293

Biogeosciences Discuss., https://doi.org/10.5194/bg-2019-11
Manuscript under review for journal Biogeosciences
Discussion started: 22 January 2019

3.4 Temperature and PAR

Correlation plots for both temperature (ºC) and sunlight (PAR) versus CH_4 emissions from the three vegetation ecotypes showed no distinct relationships with the exception of Veg B during C2 for PAR (r^2=0.18, p<0.01) and temperature (ºC) (r^2=0.35, p<0.001). No clearer trends were observed by combining all site measurements, nor separating daytime fluxes and drivers from night time fluxes and drivers.

4.0 Discussion

4.1 Geochemistry of the CASS landscape

Sediment profiles provide insights to the historical geochemical changes that have occurred across the CASS landscapes of the four Cattai Wetland sites (Fig. 5). If we assume that relatively uniform deposition of late Holocene materials occurred, the differences between present day profiles are related to historical changes in hydrology and land use, topographic elevation, geochemical trajectories and vegetative carbon inputs. For example, the permanent wetland shows distinct differences to the adjacent seasonal wetland sites, with divergent geochemical signatures of both iron and sulphate that reflect the sustained inundation (Table 1, Fig 5). The permanent wetland had significantly lower Fe(III) (p<0.001) and 11 to 30 fold lower SO_4^{2-} concentrations within the upper soil profile compared to the seasonal wetland. The ratio of $Fe(III)_{HCl}$ to $Fe(II)_{HCl}$ from the flooded soils of the permanent wetland was 0.03, indicating the sediments were almost completely depleted of Fe(III). Under reducing conditions where there is low SO_4^{2-} and little to no Fe(III) to competitively exclude methanogenesis, CH_4 production becomes more favourable. Indeed, CH_4 production was on average highest from the permanent wetland, especially when considering the duel CH_4 pathways of ebullition and air-water diffusion (Table 1).

In addition to sulphate reduction, some depletion of the sulphur pool from the permanent wetland may have occurred due to drainage exports of sulphuric acid (H_2SO_4) discharging from the CASS landscape throughout the last century. Alternatively, reducing conditions induced by re-flooding freshwater wetlands is known to encourage the re-formation of AVS and pyrite (FeS_2) and produce alkalinity, thereby attenuating acid production and discharge (Burton et al., 2007; Johnston et al., 2014; Johnston et al., 2012) and reducing the total SO_4^{2-} pool of CASS landscapes. While the AVS concentrations found within the

permanent wetland (up to 18.5 µmol g^{-1}) were a result of sulphate reduction induced by CASS wetland restoration, they nonetheless represent a relatively volatile form of sulphur, which is at risk of rapid oxidation during drought periods (Johnston et al., 2014; Karimian et al., 2017). The AVS concentrations of the permanent wetland sites were more than 20-fold higher than the three adjacent seasonal wetland sites, and represent a potentially volatile by-product and consequence of re-flooding CASS soil landscapes, in addition to leading to increases of CH_4 emissions (Table 1).

The soil profile from the seasonal wetland Veg C habitat featured abundant $Fe(III)_{HCl}$ ($Fe(III)_{HCl}$ to $Fe(II)_{HCl}$ ratio of 136) and also SO_4^{2-}. This was associated with the lowest fluxes of CH_4 for both seasonal sampling periods (Fig. 5, Table 1). Relatively low CH_4 fluxes from Veg C are likely due to the more oxidising conditions present at this site and the surfeit of thermodynamically favourable terminal electron acceptors (i.e. Fe(III) and SO_4^{2-}), which would competitively exclude organic matter degradation by methanogenic archaea (Postma & Jakobsen, 1996).

At the other seasonal wetland sites (Veg A and B), the average Fe(III) and SO_4^{2-} concentrations were intermediate, (i.e. lower than Veg C, but higher than the permanent wetland), although in the upper profile Veg B had more SO_4^{2-} while Veg A had more Fe(III) (Fig. 5, Table 1). CH_4 flux values from these sites were also intermediate (Table 1). Sediment profiles from both Veg A and Veg B indicated a degree of Fe reduction based on the ratio of Fe(III):Fe(II) which were 7.2 and 3.6 respectively. The redox potentials from Veg B during both C1 and C2 seasons (9.6 mV and -89.0 mV respectively) were consistently lower than Veg A during C1 and C2 seasons (46.5 mV and 12.0 mV respectively), which is consistent with the more reducing conditions encouraging CH_4 production in Veg B habitat. Further, as iron reduction yields more free energy than SO_4^{2-} reduction (which yields more free energy than methanogenesis) (Burdige, 2012), then Fe reduction at Veg A may outcompete CH_4 production ahead of SO_4^{2-} reduction at Veg B, which may help explain some of the differences in CH_4 production between the two sites.

Regression analysis and Spearman rho coefficients summarise the spatial trends occurring between the average sediment parameters versus seasonal CH_4 fluxes from the different sites (Fig. 7). Positive significant trends occurred for Fe(II), AVS and the $Cl:SO_4^{2-}$ ratios with CH_4 flux rates (r_s=0.88, $p<0.01$) supporting our hypothesis that reducing conditions and a smaller pool of sediment Fe(III) and SO_4^{2-} facilitate higher CH_4 production rates.

357 Alternatively, the negative trends observed between soil redox potentials, SO_4^{2-}, Fe(III) and
358 CH_4 fluxes affirm that the abundance of thermodynamically favourable terminal electron
359 acceptors plays a role in attenuating CH_4 production at each site.

360

361 **4.2 Plant-mediated CH_4 fluxes from the seasonal wetland**

362 Plant-mediated CH_4 fluxes were highest during C1 under post-dry/flooded conditions
363 with 20-30 cm of standing waters in the seasonal wetland (Table 1). While waterlogged
364 conditions are an obvious driver of higher CH_4 production rates from saturated sediments in
365 addition to the geochemical differences (previously discussed), other drivers which may
366 explain these trends include differences in diurnal variability in temperature, PAR and plant
367 physiology, which may influence CH_4 gas transport pathways.

368 In vegetated seasonal wetlands, plant-mediated gas transport is recognised as a
369 dominant pathway for CH_4 emission to the atmosphere and accounts for up to 90% of total
370 wetland fluxes (Sorrell & Boon, 1994; Whiting & Chanton, 1992). For plant survival in near-
371 permanent inundation environments, oxygen transport occurs via the araenchyma downwards
372 to the rhizome. This increases the plant performance by mitigating (i.e. oxidising) the
373 accumulation of phytotoxins such as sulphides and reducing metal ions around the roots
374 (Armstrong & Armstrong, 1990; Armstrong et al., 2006; Penhale & Wetzel, 1983). As oxygen
375 transfer to the rhizosphere occurs, an exchange of sedimentary CH_4 can be efficiently
376 transported from the rhizosphere to atmosphere, bypassing sedimentary oxidative processes
377 along the way (Fig. 8). This process in plants can be either convective (i.e. pressurised) or via
378 passive diffusive gas flow, both of which are adaptive traits of many wetland species
379 (Armstrong & Armstrong, 1991; Konnerup et al., 2011).

380 During both seasons the highest CH_4 fluxes from seasonal wetland vegetation were
381 emitted from *Phragmites australis* (Veg B) and always occurred during daylight (Table 1, Fig.
382 8). In *Phragmites australis* (Veg B), the presence of pressurised lacunar leaf culms drive a
383 mass flow of oxygen to the rhizome and back to the atmosphere via older (non-pressurised)
384 efflux culms (Henneberg et al., 2012; Sorrell & Boon, 1994). This process has been widely
385 studied in wetlands featuring this species, as it is one of the most productive and wide spread
386 flowering wetland species (Brix et al., 2001; Chanton et al., 2002; Clevering & Lissner, 1999;
387 Tucker, 1990). Kim et al. (1998) showed CH_4 emissions from *Phragmites australis* peaked
388 around midday and that daytime emissions were about 3-fold higher than night time emissions,

389 positively correlating with temperature and PAR. These were similar to our findings with
390 highest CH_4 fluxes of each seasonal time series occurring near midday (10:50 am during C1;
391 4.88 mmol m^{-2} d^{-2} and 12:15 pm during C2; 2.06 mmol m^{-2} d^{-2}) (Fig. 3). We also found a
392 positive significant relationship between CH_4 flux and both temperature and PAR during C2
393 (r^2=0.35, p<0.001 and r^2=0.18, p<0.01 respectively) (Fig. 6). The often high diurnal variability
394 in CH_4 fluxes from *Phragmites australis* occurs as convective gas transport increases
395 rhizospheric oxygen and CH_4 exchange via living culms during the daytime, whereas molecular
396 diffusion during the night time facilitates a more passive and lower CH_4 flux pathway through
397 dead culms (Armstrong & Armstrong, 1991; Chanton et al., 2002).

398 One possible reason CH_4 fluxes were lower from Veg A than Veg B despite their close
399 geographical location, may be due to the passive gas diffusion mechanism utilised by *Juncus*
400 *sp*. (Henneberg et al., 2012). Unlike the pressurised conductive gas flow mechanisms of Veg
401 B, many wetland rush species (such as Veg A) employ passive diffusive gas flow to survive
402 within water logging environments (Brix et al., 1992; Konnerup et al., 2011). Despite diffusion
403 being a less efficient gas transport mechanism (Konnerup et al., 2011), plant-mediated CH_4
404 diffusion is recognised as the dominant pathway for CH_4 emissions from many seasonal
405 wetland species. During C1 and C2, day time fluxes (diffusive) from Veg A were only 19%
406 and 33% higher than night time fluxes (diffusive). In comparison, at Veg B these day:night
407 ratios were almost triple this (67% and 94% higher) during the same periods. This may
408 potentially be due to the more efficient daytime conductive gas transfer pathway of CH_4
409 through Veg B (*Phragmites australis*) compared to the more passive diffusive CH_4 gas transfer
410 pathway of Veg A (*Juncus kraussii*). This suggests that non-pressurized pathways may result
411 in lower net rhizosphere-atmosphere gas exchange of CH_4 from seasonal wetland vegetation.

412 The *Juncus kraussii* below *Casuarina sp.* trees (Veg C) emitted nominal fluxes of CH_4
413 during both time series campaigns and was a net sink for CH_4 during C2 (Table 1, Fig. 8).
414 Although wetland trees have recently been shown to contribute significantly to CH_4 fluxes
415 from flooded environments (Pangala et al., 2017), we could not quantify or constrain the role
416 of trees as a conduit of methane to the atmosphere at this site. Regardless, there were clearly
417 lower CH_4 fluxes through the Veg C (*Juncus kraussii*) compared to the Veg A (*Juncus*
418 *kraussii*). As the species at ground level were identical, these differences are not related to
419 vegetative gas transport mechanisms, nor organic carbon content (Table 1). Shading by the
420 overhanging trees may inhibit the daytime diffusive CH_4 gas transport through Veg C
421 assumable to lower rates of photosynthesis, however PAR was only lower during C2 (Fig. 7)

and so does not appear to explain the CH_4 flux differences observed during C1. The differences are therefore likely explained by the higher positive redox potentials (Table 1) and more abundant thermodynamically favourable terminal electron acceptors (i.e. Fe(III) and SO_4^{2-}) (Fig. 5) all of which can inhibit methane production within the sediments (Burdige, 2012).

4.3 Permanent Wetland CH_4 fluxes

Diffusive CH_4 fluxes from the permanent wetland varied considerably between seasons; however, ebullition fluxes were similar (Table 1, Fig. 8). The highest seasonal CH_4 fluxes for both ebullition and diffusion (2.1 mmol m^{-2} d^{-1} and 10.5 mmol m^{-2} d^{-1} respectively) occurred during C2 despite cooler conditions (Fig. 2. Fig. 8). This however was the opposite trend to the seasonal wetland CH_4 fluxes (Table 1, Fig. 8). One reason may be due to the antecedent hydrological conditions before C1 (Fig. 2). Jeffrey et al (submitted) reported that a water level drawdown of the permanent wetland after a hot and drying summer period exposed some of the permanent wetland sediments to oxidative conditions. This may have oxidised a portion of the labile sedimentary carbon pool prior to C1 sampling of the permanent wetland, therefore reducing the total CH_4 pool observed during C1 sampling. A lag time (ranging from weeks to months) for recovery of the CH_4 pool post-drought has been observed in other systems (Boon et al., 1997) and also during lab-based experiments (Freeman et al., 1992; Knorr et al., 2008). This may explain the higher CH_4 fluxes during C2 when the system had had sufficient time to recover, despite lower water column temperatures that would normally reduce microbial metabolism rates. This hypothesis is also supported by the shift of net positive redox potential of the permanent wetland during C1 (71.7 ± 65 mV), to a strong negative redox potential during C2 (-216 ± 42 mV) indicating that there was a time lag for reducing conditions to recover within the permanent wetland for C2. This highlights the critical role of antecedent hydrological conditions and how dynamic weather oscillations of drought and floods (a common occurrence of many Australian wetland systems), strongly influence the redox potentials, soil geochemistry and ultimately CH_4 fluxes.

4.4 Implications and conclusions

Permanent wetland emissions account for the majority of the global wetland CH_4 budget however both subtropical systems and southern hemisphere systems are poorly

represented (Bartlett & Harriss, 1993; Bastviken et al., 2011) (Fig. 9). Further, the fluxes from seasonal wetlands are poorly constrained (Pfeifer-Meister et al., 2018) due to their intermittent nature and variability of intra-seasonal areal extent, which may compound why natural wetlands have the largest uncertainty of the global methane budget (Kirschke et al., 2013; Saunois et al., 2016). Although the temporal resolution of our study cannot be up scaled to realistic annual estimates, our high resolution sampling strategy provided insights to daily CH_4 flux rates revealing distinct differences between different vegetation types across the terrestrial aquatic wetland boundary. Our seasonal emissions rates were at the low end of the scale of measurements made in southern hemisphere subtropical systems but within range of northern hemisphere subtropical systems of similar latitudes (Fig. 9).

Although remediating degraded wetlands through re-flooding is a common technique to improve biodiversity, increase C sequestration and improve downstream water quality issues (Johnston et al., 2014; Johnston et al., 2004), our results propose a nuanced dilemma for land use managers, as wetland restoration can have net positive radiative forcing effects on the Earth's climate due to high rates of CH_4 production (Mitsch et al., 2013). This has also been shown to be particularly high during early remediation periods (Hemes et al., 2018). Our results suggest that seasonal wetlands emit less CH_4 on an areal basis than permanent wetlands, yet carbon accumulation in these soils may be lower (Brown et al. (in publication)). Longer-term studies over annual cycles encompassing seasonal drivers and CH_4 fluxes would further test this hypothesis of the different drivers between seasonal and permanent wetland systems.

Our results also suggest that selective hydrological restoration of wetlands featuring sediments with abundant thermodynamically favourable terminal electron acceptors (i.e. Fe(III) or SO_4^{2-}) may be a (partial) biogeochemical solution (also suggested by Hemes et al. (2018)) to both remediate degraded sites whilst simultaneously mitigating some CH_4 emissions. When Fe(III) and SO_4^{2-} are abundant in anaerobic environments they provide preferential terminal electron acceptors for microbial metabolism and thus limit methanogenesis via competitive exclusion (Achtnich et al., 1995). However, high rates of sulphate reduction coupled with Fe reduction can also lead to the accumulation of metal sulphide minerals e.g. pyrite and AVS (Johnston et al., 2014). Under permanently saturated and low oxygen conditions, metal sulphides will steadily accumulate and remain relatively benign. However, if the saturated state of remediated sites cannot be maintained, AVS may react with oxygen resulting in undesirable production of acidity and low pH conditions. Therefore the remediation of wetlands for carbon storage should involve careful site selection

to both limit CH_4 production and to avoid redox related geochemical by-products with detrimental environmental effects.

This study has highlighted how sediment geochemistry is intimately related to CH_4 production and consumption. While high sulphate and Fe(III) favour lower CH_4 production, sites featuring more reducing conditions and depleted sulphate and Fe(III) favour the highest CH_4 fluxes. Results reveal distinct differences between the areal CH_4 fluxes of four different eco-types located within a remediated subtropical Australian wetland and indicate high seasonal variability. By combining novel and well established techniques we delineated several CH_4 pathways of both seasonal and permanent wetland sources (ebullition, diffusion and plant-mediated pathways) and linked these to seasonal drivers. This provided evidence that soil geochemistry is an important factor to consider for wetland remediation in the context of CH_4 production and mitigation strategies. The CH_4 emissions results were comparable to other wetlands of similar latitudes and contribute important data for both the understudied southern hemisphere wetlands and seasonal subtropical wetland ecotypes.

Acknowledgements

We would like to thank to Roz Hagan, Bob McDonnell, Zach Ford for assistance in the field. We also thank Roz Hagan for processing the sediment cores, Isaac Santos and Ceylena Holloway for technical support and Mid Coast Council for assistance. LCJ acknowledges postgraduate support from CSIRO. This work was supported by funding from the Australian Research Council. Graphic components used in conceptual model courtesy of the Integration and Application Network, University of Maryland Centre for Environmental Science (www.ian.umces.edu/symbols).

Biogeosciences Discuss., https://doi.org/10.5194/bg-2019-11
Manuscript under review for journal Biogeosciences
Discussion started: 22 January 2019

512 **Figures**

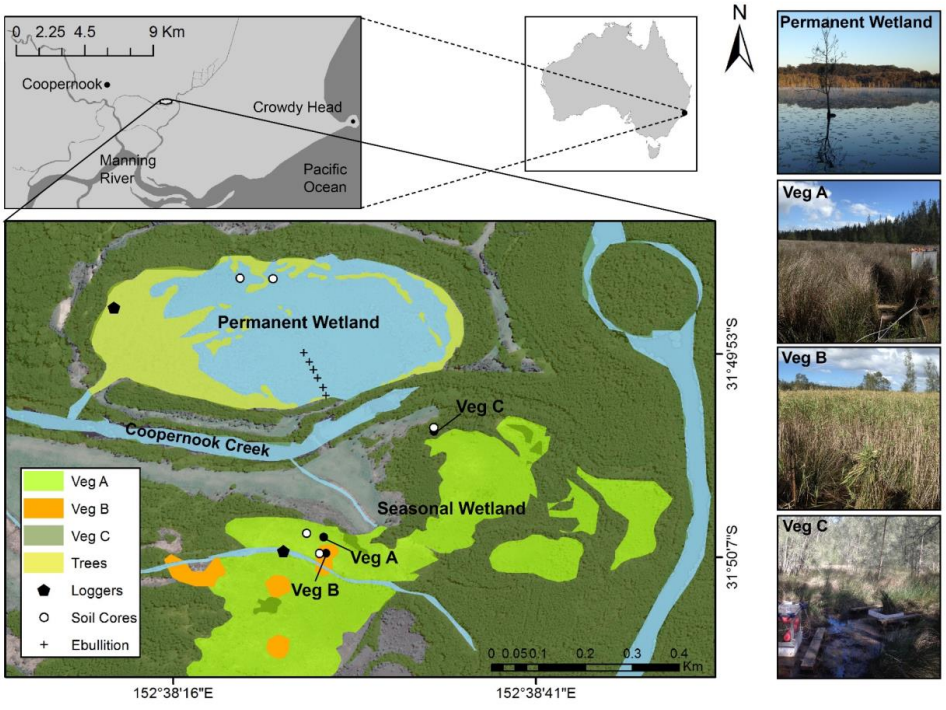

513

514 **Fig. 1** The seasonal wetland study sites consisting of Veg A (*Juncus kraussii*), Veg B
515 (*Phragmites australis*), Veg C (*Juncus kraussii* below *Casuarina sp.*) and the permanent
516 wetland indicating sediment coring sites, ebullition replicate transect, 24 h vegetation time
517 series sites and imagery of vegetation ecotypes.

518

Biogeosciences Discuss., https://doi.org/10.5194/bg-2019-11
Manuscript under review for journal Biogeosciences
Discussion started: 22 January 2019

519

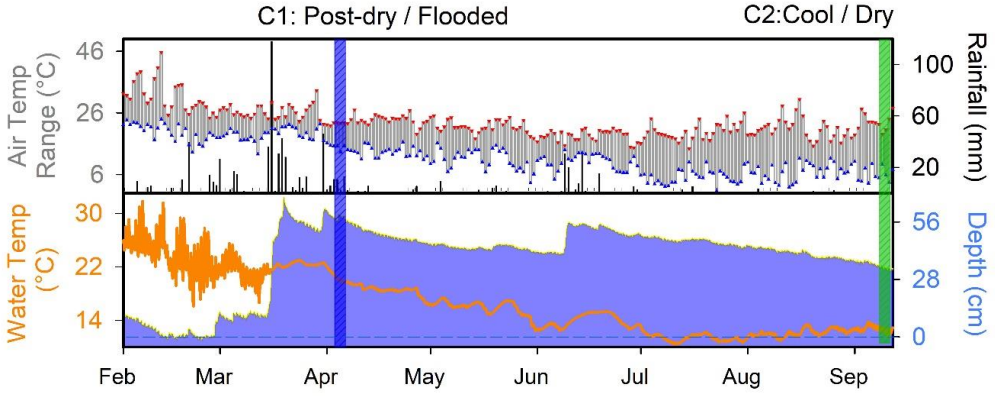

520

521 **Figure 2.** Hydrograph for the seven months of 2017 indicating daily rainfall, maximum/
522 minimum air temperature, water temperature and antecedent hydrology. Vertical coloured
523 bands represent the two fieldwork campaigns.

524

Biogeosciences Discuss., https://doi.org/10.5194/bg-2019-11
Manuscript under review for journal Biogeosciences
Discussion started: 22 January 2019

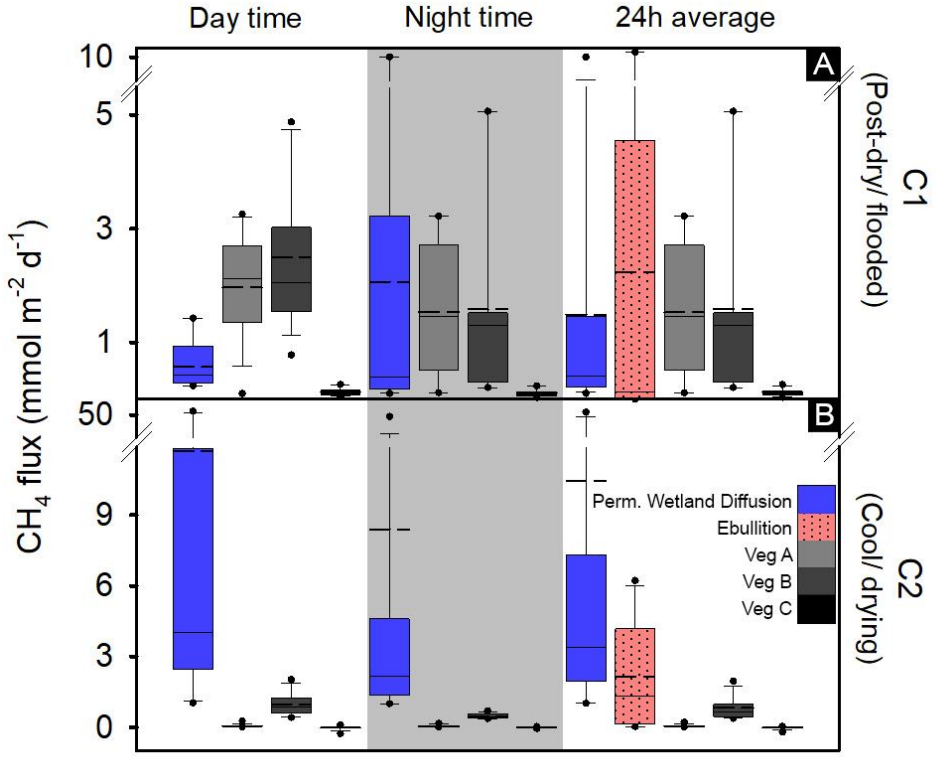

525

526 **Figure 3.** Simultaneous 24 h time series of vegetative CH_4 fluxes from the seasonal wetland
527 ecotypes at Cattai Wetland during C1: post-dry/flooded (Apr 2017) and C2: cool/drying
528 conditions (Sep 2017). The vertical error bars of the plant-mediated CH_4 flux (mmol m^{-2} d^{-1})
529 represent standard deviation of the triplicate time series measurements taken from each site and
530 horizontal bars represent the total aggregated time period represented by replicate chambers.
531 The grey shading indicates night-time. Note: Different y-axis scales for CH_4 to highlight
532 diurnal trends.

Biogeosciences Discuss., https://doi.org/10.5194/bg-2019-11
Manuscript under review for journal Biogeosciences
Discussion started: 22 January 2019

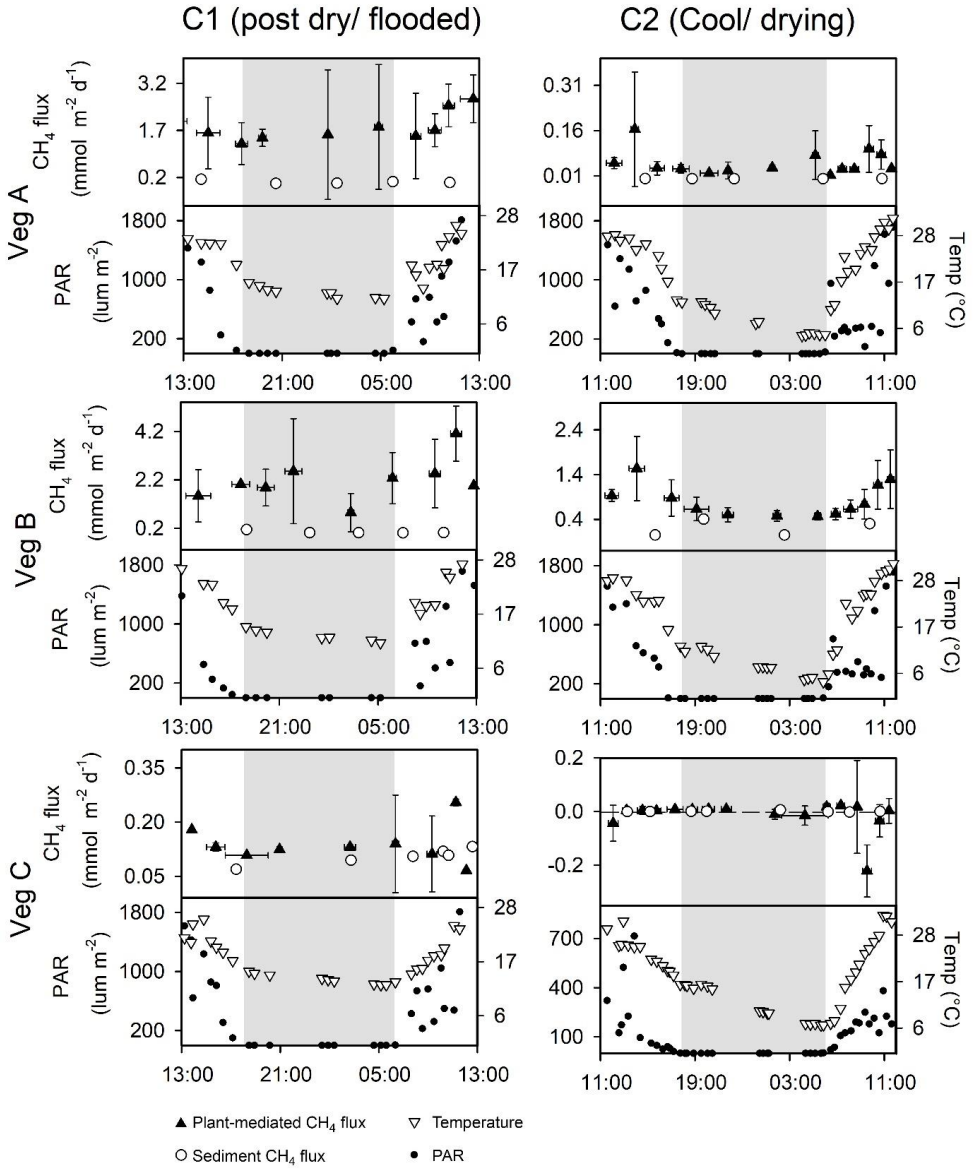

Figure 4. Seasonal fluxes of CH_4 from diurnal sampling and ebullition from the permanent wetland and adjacent 24 h time series of the seasonal wetland vegetation types A, B and C. Note: Dashed line represents the average, solid line represents the median and dots represent 5^{th} and 95^{th} percentiles.

Biogeosciences Discuss., https://doi.org/10.5194/bg-2019-11
Manuscript under review for journal Biogeosciences
Discussion started: 22 January 2019

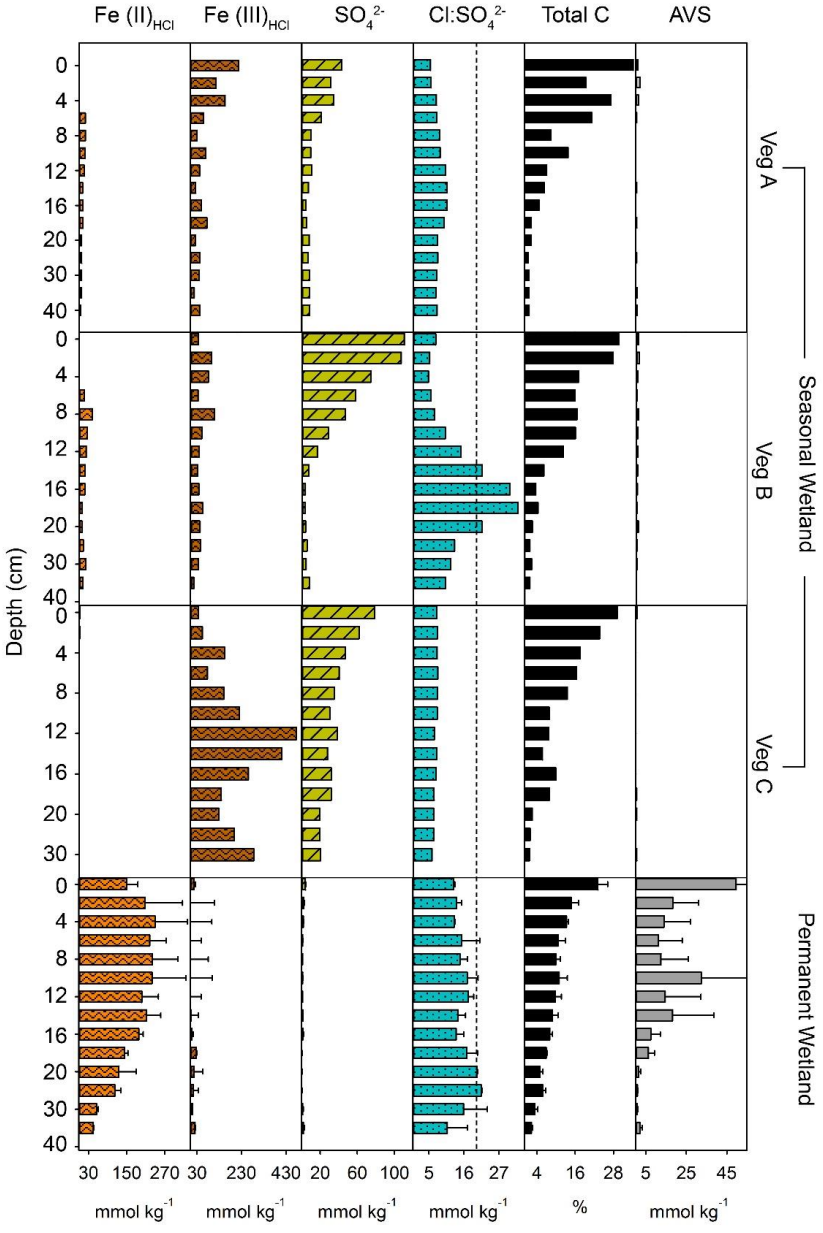

Figure 5. Soil profiles of the permanent and seasonal wetland sites indicating $Fe(II)_{HCl}$, $Fe(III)_{HCl}$, SO_4^{2-}, $Cl:SO_4^{2-}$ (a proxy for depletion of marine-derived sulphate, where >20 is broadly indicative of SO_4^{2-} reduction and <8 CASS pyrite oxidation (Mulvey, 1993)), total C and acid volatile sulphur (AVS). Note: The permanent wetland profiles are averages from two adjacent sites with error bars representing the standard deviation.

Biogeosciences Discuss., https://doi.org/10.5194/bg-2019-11
Manuscript under review for journal Biogeosciences
Discussion started: 22 January 2019

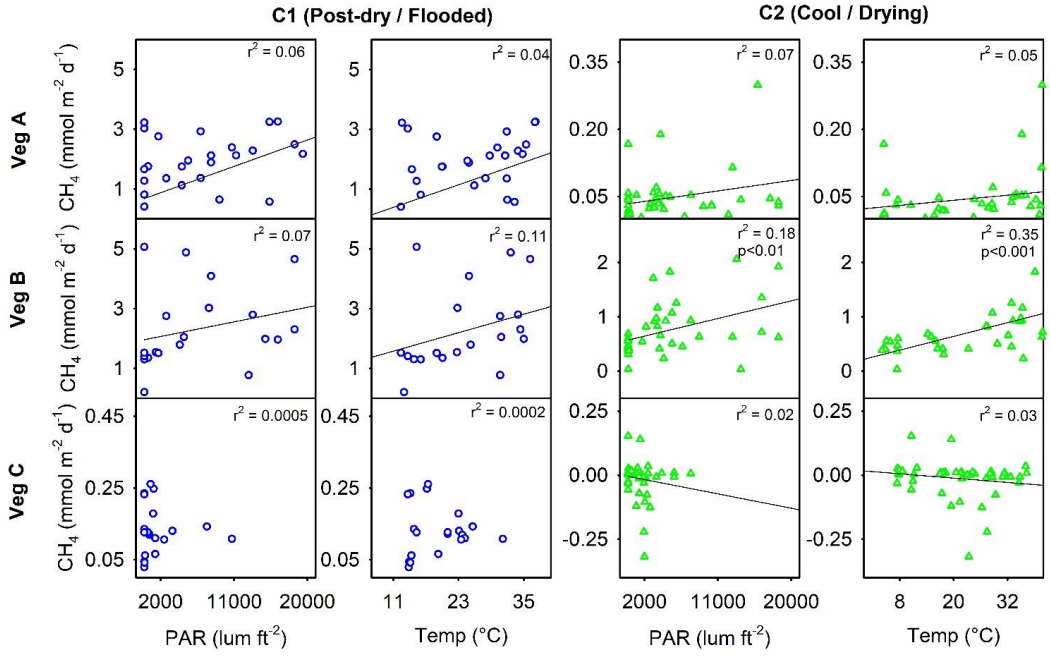

Figure 6. Correlations of CH_4 with temperature (ºC) and photo-synthetically active radiation (PAR) (lum ft^{-2}) for the three seasonal wetland vegetation sites of Cattai Wetland during two seasonal campaigns.

Biogeosciences Discuss., https://doi.org/10.5194/bg-2019-11
Manuscript under review for journal Biogeosciences
Discussion started: 22 January 2019

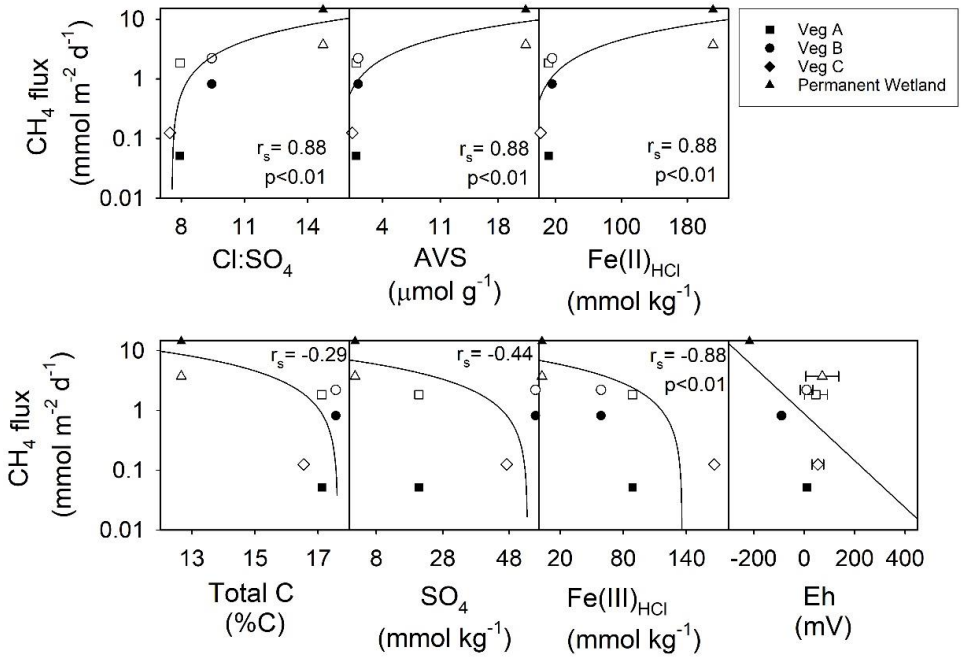

Figure 7. Regression analysis of average daily CH_4 fluxes (mmol m^{-2} d^{-1}) vs subsoil parameters of 0-20 cm core depth (i.e. CH_4 'active' zone). Note: Log scale y-axis of CH_4 fluxes from the four wetland ecotypes over two seasons. Note: The r_s values calculated using Spearman rho are for C1 (black shapes) and C2 (white shapes).

Biogeosciences Discuss., https://doi.org/10.5194/bg-2019-11
Manuscript under review for journal Biogeosciences
Discussion started: 22 January 2019

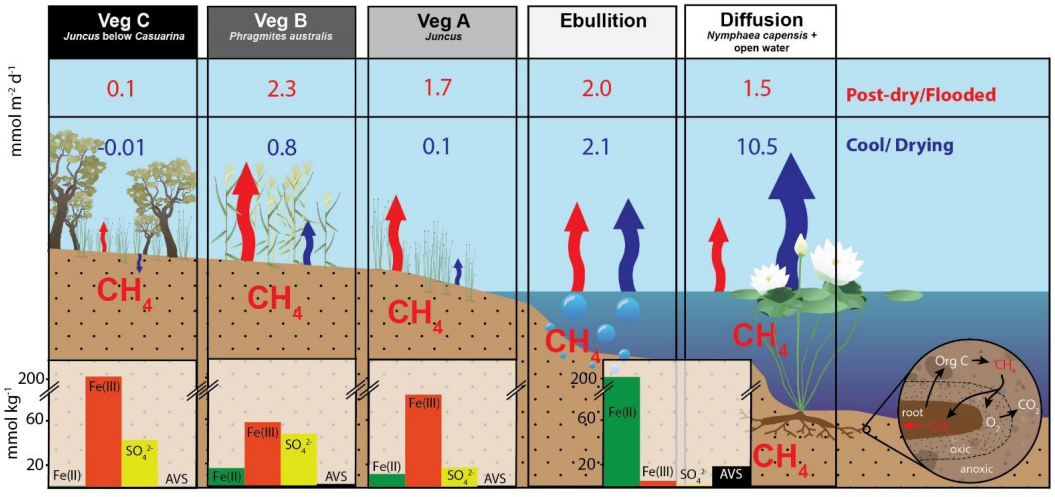

Figure 8. Conceptual model summarising the terrestrial and aquatic CH_4 fluxes (mmol m^{-2} d^{-1}) and sediment core profile parameters (mmol kg^{-1}) of the permanent and seasonal wetlands during C1 (post-dry/flooded conditions) and C2 (cool/drying conditions) of Cattai Wetland. Conceptual diagram expanded from Jeffrey et al. (in publication) and rhizome process insert adapted from (Conrad, 1993).

Biogeosciences Discuss., https://doi.org/10.5194/bg-2019-11
Manuscript under review for journal Biogeosciences
Discussion started: 22 January 2019

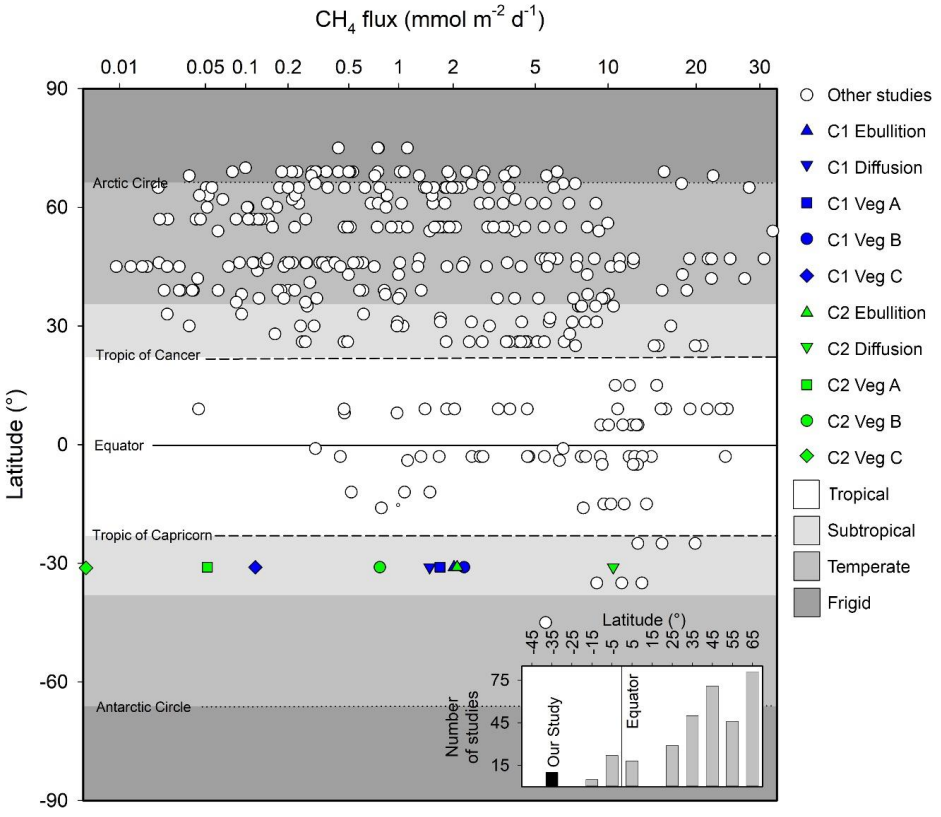

564

565 **Figure 9.** Summary of major CH_4 wetland reviews by Bartlett and Harriss (1993), Bastviken
566 et al. (2011) and modelled fluxes by Cao et al. (1998) adapted from Jeffrey et al., (in
567 publication) highlighting latitudinal trends and bias from a variety of wetland systems. Inset
568 figure highlights number of studies in these reviews by latitudinal increments of 10° poleward
569 of the equator. Note: x axis scaled to highlight subtle differences between studies.

570

571

Biogeosciences Discuss., https://doi.org/10.5194/bg-2019-11
Manuscript under review for journal Biogeosciences
Discussion started: 22 January 2019

572 **List of Tables**

573 **Table 1.** Summary of plant-mediated CH_4 fluxes from the seasonal wetland time series and
574 diurnal CH_4 fluxes and ebullition from the permanent wetland during C1 (post-dry/ flooded)
575 and C2 (cool/ drying). The corresponding sediment core data are average concentrations from
576 0 to 20 cm below ground level.

	Permanent Wetland		**Seasonal Wetland Sites**		
CH_4 flux (mmol m^{-2} d^{-1})	Ebullition	Diffusion	Veg A	Veg B	Veg C
C1 - Sediment flux			0.06	0.04	0.10
C1 - Day time		0.57	1.79	2.64	0.13
C1 - Night time		2.07	1.50	1.59	0.10
C1 - Daily average	2.02	1.49	1.70	2.27	0.12
C2 - Sediment flux			0.0004	0.20	0.0003
C2 - Day time		11.72	0.06	0.94	0.13
C2 - Night time		8.39	0.04	0.48	0.10
C2 - Daily average	2.10	10.46	0.05	0.77	-0.01
Sediment core average (0-20cm)					
Fe_{HCl} (II) (mmol kg^{-1})		202.3	11.6	15.4	1.5
Fe_{HCl} (III) (mmol kg^{-1})		5.6	83.3	56.1	204.0
SO_4^{2-} (mmol kg^{-1})		1.5	17.6	45.4	43.3
$Cl:SO_4^{2-}$		14.8	8.4	13.9	7.4
AVS (µmol g^{-1})		18.5	0.7	0.9	0.3
TOC (% C)		11.6	14.3	14.8	14.6
C1 - Redox Eh (mV)		71.7	46.5	9.6	54.4
C2 - Redox Eh (mV)		-216	12	-89	424

577

578

579

References

á Norði, K., and Thamdrup, B.: Nitrate-dependent anaerobic methane oxidation in a freshwater sediment, Geochimica et Cosmochimica Acta, 132, 141-150, 2014.

Achtnich, C., Bak, F., and Conrad, R.: Competition for electron donors among nitrate reducers, ferric iron reducers, sulfate reducers, and methanogens in anoxic paddy soil, Biology and Fertility of Soils, 19, 65-72, 1995.

ANCA: Issues paper for the Wise use Workshop, 4–6 December. Wetlands and migratory Wildlife Unit of the Australian Nature Conservation Agency, Canberra. 42 pp, 1995.

Armentano, T., and Menges, E.: Patterns of change in the carbon balance of organic soil-wetlands of the temperate zone, The Journal of Ecology, 755-774, 1986.

Armstrong, J., and Armstrong, W.: Light-enhanced convective throughflow increases oxygenation in rhizomes and rhizosphere of Phragmites australis (Cav.) Trin. ex Steud, New Phytologist, 114, 121-128, 1990.

Armstrong, J., and Armstrong, W.: A convective through-flow of gases in Phragmites australis (Cav.) Trin. ex Steud, Aquatic Botany, 39, 75-88, 1991.

Armstrong, J., Jones, R., and Armstrong, W.: Rhizome phyllosphere oxygenation in Phragmites and other species in relation to redox potential, convective gas flow, submergence and aeration pathways, New Phytologist, 172, 719-731, 2006.

Association, A. P. H., Association, A. W. W., Federation, W. P. C., and Federation, W. E.: Standard methods for the examination of water and wastewater, American Public Health Association., 1915.

Bartlett, K. B., and Harriss, R. C.: Review and assessment of methane emissions from wetlands, Chemosphere, 26, 261-320, 1993.

Bastviken, D., Tranvik, L. J., Downing, J. A., Crill, P. M., and Enrich-Prast, A.: Freshwater methane emissions offset the continental carbon sink, Science, 331, 50,2011.

Bianchi, T. S.: Biogeochemistry of estuaries, Oxford University Press New York, 2007.

Boman, A., Åström, M., and Fröjdö, S.: Sulfur dynamics in boreal acid sulfate soils rich in metastable iron sulfide—the role of artificial drainage, Chemical Geology, 255, 68-77, 2008.

Boon, P. I., Mitchell, A., and Lee, K.: Effects of wetting and drying on methane emissions from ephemeral floodplain wetlands in south-eastern Australia, Hydrobiologia, 357, 73-87, 1997.

612 Bridgham, S. D., Moore, T. R., Richardson, C. J., and Roulet, N. T.: Errors in greenhouse
613 forcing and soil carbon sequestration estimates in freshwater wetlands: a comment on
614 Mitsch et al. (2013), Landscape Ecology, 29, 1481-1485, 2014.
615 Brix, H., Sorrell, B. K., and Orr, P. T.: Internal pressurization and convective gas flow in
616 some emergent freshwater macrophytes, Limnology and Oceanography, 37, 1420-1433,
617 1992.
618 Brix, H., Sorrell, B. K., and Lorenzen, B.: Are Phragmites-dominated wetlands a net source
619 or net sink of greenhouse gases?, Aquatic Botany, 69, 313-324, 2001.
620 Burdige, D.: Estuarine and coastal sediments–coupled biogeochemical cycling, Treatise on
621 Estuarine and Coastal Science, 5, 279-316, 2012.
622 Burton, E., Bush, R. T., Johnston, S. G., Sullivan, L. A., and Keene, A. F.: Sulfur
623 biogeochemical cycling and novel Fe–S mineralization pathways in a tidally re-flooded
624 wetland, Geochimica et Cosmochimica Acta, 75, 3434-3451, 2011.
625 Burton, E. D., Bush, R. T., and Sullivan, L. A.: Elemental sulfur in drain sediments
626 associated with acid sulfate soils, Applied Geochemistry, 21, 1240-1247, 2006.
627 Burton, E. D., Bush, R. T., Sullivan, L. A., and Mitchell, D. R. G.: Reductive transformation
628 of iron and sulfur in schwertmannite-rich accumulations associated with acidified
629 coastal lowlands, Geochimica et Cosmochimica Acta, 71, 4456-4473,
630 10.1016/j.gca.2007.07.007, 2007.
631 Cao, M., Gregson, K., and Marshall, S.: Global methane emission from wetlands and its
632 sensitivity to climate change, Atmospheric environment, 32, 3293-3299, 1998.
633 Chanton, J. P., Arkebauer, T. J., Harden, H. S., and Verma, S. B.: Diel variation in lacunal
634 CH 4 and CO 2 concentration and δ 13 C in Phragmites australis, Biogeochemistry, 59,
635 287-301, 2002.
636 Claff, S. R., Sullivan, L. A., Burton, E. D., and Bush, R. T.: A sequential extraction
637 procedure for acid sulfate soils: partitioning of iron, Geoderma, 155, 224-230, 2010.
638 Clevering, O. A., and Lissner, J.: Taxonomy, chromosome numbers, clonal diversity and
639 population dynamics of Phragmites australis, Aquatic Botany, 64, 185-208, 1999.
640 Conrad, R.: Mechanisms controlling methane emission from wetland rice fields, in:
641 Biogeochemistry of Global Change, Springer, 317-335, 1993.
642 Costanza, R., de Groot, R., Sutton, P., van der Ploeg, S., Anderson, S. J., Kubiszewski, I.,
643 Farber, S., and Turner, R. K.: Changes in the global value of ecosystem services,
644 Global Environmental Change, 26, 152-158, 2014.

Deverel, S. J., Ingrum, T., and Leighton, D.: Present-day oxidative subsidence of organic soils and mitigation in the Sacramento-San Joaquin Delta, California, USA, Hydrogeology journal, 24, 569-586, 2016.

Finlayson, C. M., and Rea, N.: Reasons for the loss and degradation of Australian wetlands, Wetlands Ecology and Management, 7, 1-11, 1999.

Freeman, C., Lock, M., and Reynolds, B.: Fluxes of CO_2, CH_4 and N_2O from a Welsh peatland following simulation of water table draw-down: Potential feedback to climatic change, Biogeochemistry, 19, 51-60, 1992.

Hemes, K. S., Chamberlain, S. D., Eichelmann, E., Knox, S. H., and Baldocchi, D. D.: A biogeochemical compromise: The high methane cost of sequestering carbon in restored wetlands, Geophysical Research Letters, 45, 6081-6091, 2018.

Henneberg, A., Sorrell, B. K., and Brix, H.: Internal methane transport through Juncus effusus: experimental manipulation of morphological barriers to test above-and below-ground diffusion limitation, New Phytologist, 196, 799-806, 2012.

Holmkvist, L., Ferdelman, T. G., and Jørgensen, B. B.: A cryptic sulfur cycle driven by iron in the methane zone of marine sediment (Aarhus Bay, Denmark), Geochimica et Cosmochimica Acta, 75, 3581-3599, 2011.

Jeffrey, L. C., Maher, D. T., Santos, I. R., McMahon, A., and Tait, D. R.: Groundwater, Acid and Carbon Dioxide Dynamics Along a Coastal Wetland, Lake and Estuary Continuum, Estuaries and Coasts, 39, 1325-1344, 2016.

Johnston, S. G., Slavich, P. G., Sullivan, L. A., and Hirst, P.: Artificial drainage of floodwaters from sulfidic backswamps: effects on deoxygenation in an Australian estuary, Marine and Freshwater Research, 54, 781-795, 2003.

Johnston, S. G., Slavich, P. G., and Hirst, P.: The effects of a weir on reducing acid flux from a drained coastal acid sulphate soil backswamp, Agricultural Water Management, 69, 43-67, 2004.

Johnston, S. G., Keene, A. F., Burton, E. D., Bush, R. T., and Sullivan, L. A.: Quantifying alkalinity generating processes in a tidally remediating acidic wetland, Chemical Geology, 304, 106-116, 2012.

Johnston, S. G., Burton, E. D., Aaso, T., and Tuckerman, G.: Sulfur, iron and carbon cycling following hydrological restoration of acidic freshwater wetlands, Chemical Geology, 371, 9-26, 2014.

677 Karimian, N., Johnston, S. G., and Burton, E. D.: Acidity generation accompanying iron and
678 sulfur transformations during drought simulation of freshwater re-flooded acid sulfate
679 soils, Geoderma, 285, 117-131, 2017.
680 Karimian, N., Johnston, S. G., and Burton, E. D.: Iron and sulfur cycling in acid sulfate soil
681 wetlands under dynamic redox conditions: A review, Chemosphere, 197, 803-816,
682 10.1016/j.chemosphere.2018.01.096, 2018.
683 Kim, J., Verma, S., Billesbach, D., and Clement, R.: Diel variation in methane emission from
684 a midlatitude prairie wetland: significance of convective throughflow in Phragmites
685 australis, Journal of Geophysical Research: Atmospheres, 103, 28029-28039, 1998.
686 Kirschke, S., Bousquet, P., Ciais, P., Saunois, M., Canadell, J. G., Dlugokencky, E. J.,
687 Bergamaschi, P., Bergmann, D., Blake, D. R., Bruhwiler, L., Cameron-Smith, P.,
688 Castaldi, S., Chevallier, F., Feng, L., Fraser, A., Heimann, M., Hodson, E. L.,
689 Houweling, S., Josse, B., Fraser, P. J., Krummel, P. B., Lamarque, J.-F., Langenfelds,
690 R. L., Le Quéré, C., Naik, V., O'Doherty, S., Palmer, P. I., Pison, I., Plummer, D.,
691 Poulter, B., Prinn, R. G., Rigby, M., Ringeval, B., Santini, M., Schmidt, M., Shindell,
692 D. T., Simpson, I. J., Spahni, R., Steele, L. P., Strode, S. A., Sudo, K., Szopa, S., van
693 der Werf, G. R., Voulgarakis, A., van Weele, M., Weiss, R. F., Williams, J. E., and
694 Zeng, G.: Three decades of global methane sources and sinks, Nature Geoscience, 6,
695 813-823, 10.1038/ngeo1955, 2013.
696 Knorr, K.-H., Glaser, B., and Blodau, C.: Fluxes and 13 C isotopic composition of dissolved
697 carbon and pathways of methanogenesis in a fen soil exposed to experimental drought,
698 Biogeosciences Discussions, 5, 1319-1360, 2008.
699 Konnerup, D., Sorrell, B. K., and Brix, H.: Do tropical wetland plants possess convective gas
700 flow mechanisms?, New Phytol, 190, 379-386, 10.1111/j.1469-8137.2010.03585.x,
701 2011.
702 Lal, R.: Carbon sequestration, Philosophical Transactions of the Royal Society of London B:
703 Biological Sciences, 363, 815-830, 2008.
704 Melton, J., Wania, R., Hodson, E., Poulter, B., Ringeval, B., Spahni, R., Bohn, T., Avis, C.,
705 Beerling, D., and Chen, G.: Present state of global wetland extent and wetland methane
706 modelling: conclusions from a model intercomparison project (WETCHIMP),
707 Biogeosciences, 10, 753-788, 2013.
708 Mitsch, W. J., Bernal, B., Nahlik, A. M., Mander, Ü., Zhang, L., Anderson, C. J., Jørgensen,
709 S. E., and Brix, H.: Wetlands, carbon, and climate change, Landscape Ecology, 28,
710 583-597, 2013.

Mulvey, P.: Pollution, prevention and management of sulphidic clays and sands. Proceedings National Conference on Acid Sulphate Soils. (Ed. R Bush) pp, 116-129, 1993.

Nedwell, D. B., and Watson, A.: CH4 production, oxidation and emission in a UK ombrotrophic peat bog: influence of SO42− from acid rain, Soil Biology and Biochemistry, 27, 893-903, 1995.

Neubauer, S. C., and Megonigal, J. P.: Moving beyond global warming potentials to quantify the climatic role of ecosystems, Ecosystems, 18, 1000-1013, 2015.

Page, K., and Dalal, R.: Contribution of natural and drained wetland systems to carbon stocks, CO2, N2O, and CH4 fluxes: an Australian perspective, Soil Research, 49, 377-388, 2011.

Pangala, S. R., Enrich-Prast, A., Basso, L. S., Peixoto, R. B., Bastviken, D., Hornibrook, E. R., Gatti, L. V., Marotta, H., Calazans, L. S. B., and Sakuragui, C. M.: Large emissions from floodplain trees close the Amazon methane budget, Nature, 552, 230, 2017.

Penhale, P. A., and Wetzel, R. G.: Structural and functional adaptations of eelgrass (Zostera marina L.) to the anaerobic sediment environment, Canadian Journal of Botany, 61, 1421-1428, 1983.

Pereyra, A. S., and Mitsch, W. J.: Methane emissions from freshwater cypress (Taxodium distichum) swamp soils with natural and impacted hydroperiods in Southwest Florida, Ecological Engineering, 114, 46-56, 2018.

Pfeifer-Meister, L., Gayton, L. G., Roy, B. A., Johnson, B. R., and Bridgham, S. D.: Greenhouse gas emissions limited by low nitrogen and carbon availability in natural, restored, and agricultural Oregon seasonal wetlands, PeerJ, 6, 10.7717/peerj.5465, 2018.

Poffenbarger, H. J., Needelman, B. A., and Megonigal, J. P.: Salinity influence on methane emissions from tidal marshes, Wetlands, 31, 831-842, 2011.

Postma, D., and Jakobsen, R.: Redox zonation: equilibrium constraints on the Fe (III)/SO4-reduction interface, Geochimica et Cosmochimica Acta, 60, 3169-3175, 1996.

Rayment, G., and Higginson, F. R.: Australian laboratory handbook of soil and water chemical methods, Inkata Press Pty Ltd, 1992.

Sammut, J., White, I., and Melville, M.: Acidification of an estuarine tributary in eastern Australia due to drainage of acid sulfate soils, Marine and Freshwater Research, 47, 669-684, 1996.

743 Saunois, M., Bousquet, P., Poulter, B., Peregon, A., Ciais, P., Canadell, J. G., Dlugokencky,
744 E. J., Etiope, G., Bastviken, D., and Houweling, S.: The global methane budget 2000–
745 2012, Earth System Science Data (Online), 8, 2016.
746 Sivan, O., Antler, G., Turchyn, A. V., Marlow, J. J., and Orphan, V. J.: Iron oxides stimulate
747 sulfate-driven anaerobic methane oxidation in seeps, Proceedings of the National
748 Academy of Sciences, 111, E4139-E4147, 2014.
749 Sorrell, B. K., and Boon, P. I.: Convective gas flow in Eleocharis sphacelata R. Br.: methane
750 transport and release from wetlands, Aquatic Botany, 47, 197-212, 1994.
751 Tucker, G. C.: The genera of Arundinoideae (Gramineae) in the southeastern United States,
752 Journal of the Arnold Arboretum, 71, 145-177, 1990.
753 Tulau, M.: Acid Sulphate Soil Priority Management Areas on the Lower Hastings Camden
754 Haven Floodplains, Department of Land and Water Conservation, 1999.
755 Villa, J. A., and Bernal, B.: Carbon sequestration in wetlands, from science to practice: An
756 overview of the biogeochemical process, measurement methods, and policy framework,
757 Ecological Engineering, 114, 115-128, 10.1016/j.ecoleng.2017.06.037, 2018.
758 Walker, P. H.: Seasonal and stratigraphic controls in coastal floodplain soils, Soil Research,
759 10, 127-142, 1972.
760 White, I., Melville, M., Wilson, B., and Sammut, J.: Reducing acidic discharges from coastal
761 wetlands in eastern Australia, Wetlands Ecology and Management, 5, 55-72, 1997.
762 Whiting, G. J., and Chanton, J. P.: Plant-dependent CH4 emission in a subarctic Canadian
763 fen, Global biogeochemical cycles, 6, 225-231, 1992.
764 Whiting, G. J., and Chanton, J. P.: Greenhouse carbon balance of wetlands: methane emission
765 versus carbon sequestration, Tellus B: Chemical and Physical Meteorology, 53, 521-
766 528, 2001.
767 Wong, V. N., Johnston, S. G., Bush, R. T., Sullivan, L. A., Clay, C., Burton, E. D., and
768 Slavich, P. G.: Spatial and temporal changes in estuarine water quality during a post-
769 flood hypoxic event, Estuarine, Coastal and Shelf Science, 87, 73-82, 2010.

770